Simplified Procedure for Estimating Epitaxy of $La_2Zr_2O_7$-Buffered NiW RABITS Using XRD

Mark O. Rikel, Dirk Isfort, Marcel Klein, Jürgen Ehrenberg, Joachim Bock, Elliot D. Specht, Ming Sun-Wagener, Oxana Weber, Dieter Sporn, Sebastian Engel, Oliver de Haas, Robert Semerad, Margitta Schubert, and Bernhard Holzapfel

***Abstract*—A procedure is developed for assessing the epitaxy of $La_{2-x}Zr_{2+x}O_7$ (LZO) layers on NiW RABITS. Comparing XRD patterns ($\theta - 2\theta$ scans and 2D rocking curves) of LZO films of known thickness (ellipsometry or reflectometry measurements) with those of standard samples (100% epitaxial LZO film and an isotropic LZO pellet of known density), we estimate the epitaxial (EF), and polycrystalline (PF) fractions of LZO within the layer. The procedure was tested using MOD-LZO(100 nm)/NiW tape samples with EF varied from 3 to 90% (reproducibly prepared by varying the humidity of $Ar - 5\%H_2$ gas during heat treatment). A qualitative agreement with RHEED and quantitative (within $\pm 10\%$) agreement with the EBSD results was shown. Correlation between EF and J_c in 600 nm thick YBCO layer deposited on MOD-LZO/NiW using thermal coevaporation enables us to impose the $EF = 80\%$ margin on the quality of LZO layer for the particular conductor architecture.**

***Index Terms*—Epitaxial layers, quality control, x-ray measurements.**

I. Introduction

QUALITY control of intermediate buffer layers in coated conductors (CC) is a necessary prerequisite for a stable fabrication process of long lengths [1]. Efficient control requires development of quantitative criteria for all essential layer properties and imposing quality margins on those criteria through analysis of their correlation with the final performance. In this contribution, we present an example of such an approach with respect to epitaxy of $La_{2-x}Zr_{2+x}O_7$ (LZO) layers deposited on NiW RABITS using metalorganic deposition., economically the most promising route for fabricating buffered substrates [2].

Epitaxy of buffer layers in RABITS based coated conductors is one of the most essential properties that requires rigorous control. The quantitative texture characterization by XRD pole figure measurements has been applied for continuous quality control of 20 m long lengths [3]. In this work, we developed a simplified procedure potentially applicable to characterization of longer lengths. The procedure is based on comparing XRD data for the sample in question and reference samples in order to quantitatively assess the epitaxial and polycrystalline fractions within the layer. In this paper, we present the results of testing the procedure using EBSD and RHEED, discuss correlation between the estimated EF values and the critical current density J_c in 10 cm long CC samples with the one buffer layer architecture, PVD-YBCO/MOD-LZO/NiW, and consequences of this correlation to the quality control of the LZO layer.

II. Experimental

Ni-5%W metallic substrates with 98% cube texture were supplied by the evico GmbH. LZO layers were deposited by dip coating. A 0.45 M La- and Zr-acac solution with propionic acid as a solvent was used. For most of the experiments described below, 10 m long NiW tape was dip coated and dried in a prototype reel-to-reel (RTR) system; 10 cm long samples were then cut and heat treated using a two step process (Fig. 1) in $Ar - 5\%H_2$ gas flow saturated with water vapor to different humidity levels (dew point $DP = -45$ to $-5°C$). The LZO powder was prepared by drying the same precursor solution and calcining it at 1000°C. A pressed pellet was then annealed at 1100°C in $Ar - 5\%H_2$.

600 nm thick YBCO films were deposited by thermal coevaporation on LZO/NiW tapes held at 680°C with a growth rate 0.3 nm/s (see [4] for details). J_c (77 K, sf) were measured inductively using Cryoscan (Theva GmbH).

Thickness of LZO layers was determined by reflectometry (NanoCalc) and ellipsometry (SOPRA). For the 50 to 170 nm thick LZO films studied, the results of the two methods coincide within 3% with SEM measurements on the FIB cuts.

XRD measurements were made using a D5000 four-circle diffractometer (Cu $K\alpha$ radiation; resolution: $\sim 0.2°$ in ω and $\sim 2.5°$ in χ). RHEED patterns were measured using a Staib Instrument System. EBSD measurements were made using a Leo-Gemini1530 with an Nordlys II EBSD-detector.

Manuscript received August 15, 2008. First published June 30, 2009; current version published July 15, 2009. The work was supported in part by BMBF within the WING program (project SupraNanoSol) and by the US DOE, Office of Electricity Delivery and Energy Reliability. Corresponding author: M. O. Rikel (e-mail: Mark.Rikel@Nexans.com).

M. O. Rikel, M. Klein, J. Ehrenberg and J. Bock are with Nexans SuperConductors, Chemiepark Knapsack, D-50354 Germany (e-mail: Mark.Rikel@Nexans.com).

D. Isfort was with Nexans SuperConductors until 2007.

E. D. Specht is with Oak Ridge National Lab (e-mail: spechted@ornl.gov).

M. Sun-Wagener, O. Weber, and D. Sporn are with Fraunhofer-Institut für Silicatforschung ISC, D-97082 Würzburg, Germany (e-mail: Ming.Sun-Wagener@isc.fraunhofer.de).

S. Engel and O. de Haas are with evico GmbH, D-01069 Dresden, Germany (e-mail: deHaas@evico.de).

R. Semerad is with Theva Dünnschichttechnik GmbH, 85737 Ismaning, Germany (e-mail: semerad@theva.com).

M. Schubert and B. Holzapfel are with IFW Dresden, D-01171 Dresden, Germany (e-mail: B.Holzapfel@ifw-dresden.de).

Color versions of one or more of the figures in this paper are available online at http://ieeexplore.ieee.org.

Digital Object Identifier 10.1109/TASC.2009.2017907

1051-8223/$25.00 © 2009 IEEE

Authorized licensed use limited to: Oak Ridge National Laboratory. Downloaded on September 6, 2009 at 11:04 from IEEE Xplore. Restrictions apply.

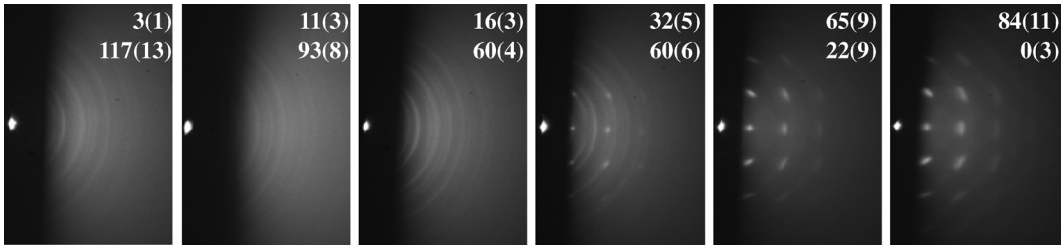

Fig. 3. RHEED patterns of samples with different percentage of epitaxial and polycrystalline LZO shown as upper and bottom figures, respectively.

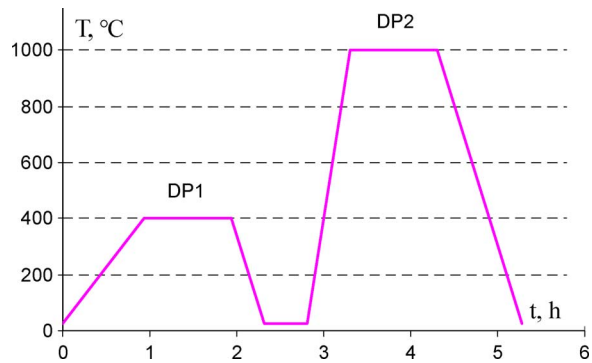

Fig. 1. Time temperature profile of heat treating LZO-gel layers on NiW samples in $\mathrm{Ar}-5\%\mathrm{H}_2$ saturated with $\mathrm{H}_2\mathrm{O}$ vapor to humidity corresponding to the dew points DP varied from -45 to $-5\,^{\circ}\mathrm{C}$.

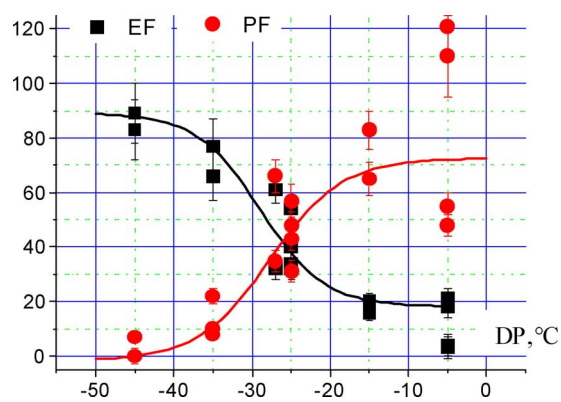

Fig. 2. Effect of humidity of processing atmosphere $(\mathrm{Ar}-5\%\mathrm{H}_2)$ during heat treatment on epitaxial (EF) and polycrystalline (PF) fractions of LZO (the data for heat treatment of Fig. 1 with dew points $\mathrm{DP1} = \mathrm{DP2} = \mathrm{DP}$).

III. Estimation of Epitaxial and Polycrystalline Fractions in LZO Layer From XRD Data

Epitaxial (EF) and polycrystalline (PF) fractions in thin LZO films of thickness d are determined by comparing the characteristics of 400 and 222 reflections of the sample in question (subscript S) and a reference, that is, either a perfect sample (subscript P) with 100% epitaxial LZO in case of EF determination or an isotropic pressed pellet of known relative density (η) in case of PF determination. The formulas used are (see Appendix for clarification and notations)

$$EF_{400} = \gamma \frac{A_{400}^{S}\left\{1-\exp(-2\mu d_P/\sin(\theta)\right\}\Delta\omega_S^{RD}\Delta\omega_S^{TD}}{A_{400}^{P}\left\{1-\exp[-2\mu d_S/\sin(\theta)\right\}\Delta\omega_P^{RD}\Delta\omega_P^{TD}} \quad (1)$$

TABLE I
Comparison of EF Data (%) Obtained From XRD and EBSD

XRD	EBSD
32(5)	26(5)
65(9)	85(5)
84(11)	90(4)

$$PF_{222} = \gamma A_{222}^{S} / \left\{ A_{222}^{pellet} \times [1-\exp(-2\mu d_S/\sin\theta)] \times \eta \right\} \quad (2)$$

An LZO-coated NiW sample with only spot reflections in the RHEED pattern was chosen as a reference P. The EF values obtained from (1) were first considered as normalized characteristics of the epitaxy measured in arbitrary units. During the two-year experience of using the procedure as a quality control tool, the reference P was changed twice when obtaining samples with $EF > 110\%$.

IV. Testing the Procedure

Fig. 2 shows variation of EF and PF in LZO layers formed on NiW tapes annealed according to Fig. 1 in the $\mathrm{Ar}-5\%\mathrm{H}_2$ gas flow saturated with water vapor to different humidity levels (this is different from the known effect of humidity during deposition reported earlier [5]). Increasing the humidity is clearly favorable for nucleation and growth of randomly oriented grains. Six samples from this series with $\mathrm{EF} = 3-90\%$ were chosen for RHEED measurements of which three with $\mathrm{EF} > 30\%$ were also characterized by EBSD.

A. Epitaxial Fraction EF

The RHEED patterns of the samples with various EF and PF values are presented in Fig. 3 showing a very good qualitative agreement with the XRD data.

Table I compares the EF data obtained by XRD and EBSD. Within the statistical error, both methods give the same results.

As EBSD measurements probe a layer a few nanometer thick, while XRD measurements probe the whole film thickness, the coincidence of the data of the two methods within the 15% relative accuracy suggests that in the particular samples (LZO formed under various humidity conditions) all epitaxial grains grow through the whole layer thickness.

B. Polycrystalline Fraction PF

Accuracy of determining PF according to (2) strongly depends on the presence of preferred orientation in the film. A fiber

Authorized licensed use limited to: Oak Ridge National Laboratory. Downloaded on September 6, 2009 at 11:04 from IEEE Xplore. Restrictions apply.

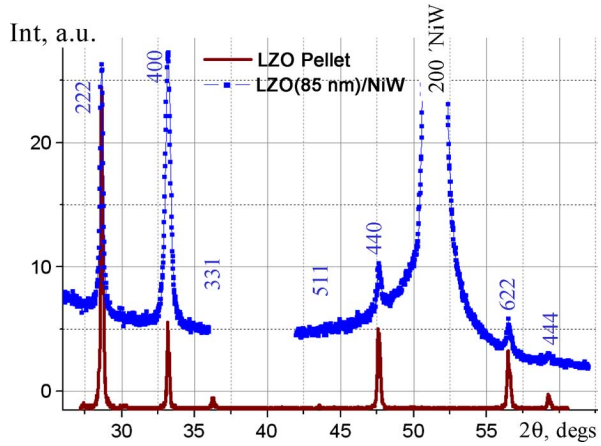

Fig. 4. XRD patterns of LZO pellet and LZO film on NiW with $EF = 11 \pm 4\%$ and $PF = 121 \pm 13\%$. The patterns are normalized to the same area of the 222 peak of LZO. Difference in penetration depths of x-rays is taken into account by modifying the intensity of the pellet as $I(2\theta) = I_0(2\theta)[1 - \exp(-2\mu d//\sin(\theta)]$, where μ is the absorption coefficient of LZO, d the layer thickness (85 nm).

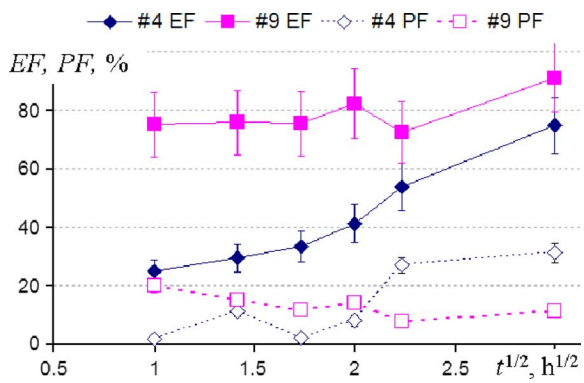

Fig. 5. EF and PF data versus cumulative time of successive annealing treatments of LZO(100 nm)/NiW at 1000°C in $Ar - 5\%H_2$ flow with humidity corresponding to $DP = -35°C$ for the first three and $+5°C$ for the last two treatments. Samples #4 and #9 were cut from different positions of 10 m long tape continuously crystallized (1 h at 1000°C) in the RTR system.

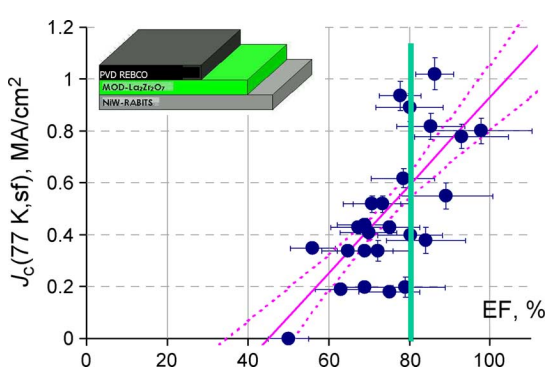

Fig. 6. Jc(77 K, sf) in 600 nm thick e-beam YBCO films deposited on Ni5%W RABITS MOD coated with 70 to 160 nm thick LZO layer as function of epitaxial fraction EF of LZO.

111 texture component is rarely observed in LZO/NiW; then estimates of PF are unrealistically high. Such cases require special analysis.[1] In most (99%) samples, however, and particularly in those studied in this work, the preferred orientation is small. As an example, Fig. 4 compares XRD patterns for the isotropic LZO pellet and the sample heat treated in a humid $Ar - 5\%H_2$ ($DP = -5°C$) with the calculated $PF = 121 \pm 13\%$. The intensities of the two patterns are normalized to have the same areas under 222 peaks and take into account the difference in penetration depths of x-rays at different 2θ. The non-$h00$ peaks of the LZO film are somewhat smaller than those of the pellet, which indicates a slight 111 preferred orientation. Estimates of the preferred orientation parameter PO using March function approach [6] gave $PO = 0.82 \pm 0.04$, so that the PF value is overestimated by a factor of $PO^{-3} = 1.82 \pm 0.26$, and the real $PF = 67 \pm 12\%$.

C. Amorphous Fraction

Despite of the possibly large errors, estimates of PF given by (2) are nevertheless practically useful. For example, it follows from Fig. 2 that within the experimental accuracy the sum $EF + PF \approx 1$ for most samples. When this is observed, subsequent annealing of samples did not result in changes of EF and PF (Fig. 5; sample #9). On the contrary, in case of $EF + PF < 1$, so that the layer presumably contains amorphous phase in the amount $AF = 1 - EF - PF$, subsequent annealing the samples leads to further crystallization until $EF + PF = 1$ (Fig. 5: sample #4).[2]

V. Correlation Between Jc and Epitaxial Fraction of LZO in PVD-YBCO/MOD-LZO/Ni-5%W Rabits

In Fig. 6, we plot the results of J_c measurements in 600 nm thick YBCO films deposited on 70 to 160 nm thick LZO-coated Ni-5%W as function of epitaxial fraction of LZO layer (note that within 10% accuracy J_c was found independent of the LZO layer thickness). A strong correlation between J_c and EF is observed. For $EF < 60\%$, $J_c \approx 0$. For $EF > 60\%$, a large scatter in J_c is observed, though there is a clear tendency of increasing J_c with increasing EF. As in most of our samples, the estimated EF represents the fraction of grains epitaxially grown to the surface through the whole layer thickness, the correlation of Fig. 6 can be roughly interpreted in terms of percolation behavior, i.e., for $EF < 65\%$, there always exists a continuous current breaking path, and $J_c \approx 0$.

VI. Application to Quality Control of the LZO Layer

Though the epitaxial fraction of LZO is obviously not the only factor influencing J_c, it is a useful characteristic for the quality control of the LZO layer. The vertical line in Fig. 6 at $EF = 80\%$ roughly separates the region of small and unstable performance from that of rather reproducible J_c. The $EF = 80\%$ is (conditionally) chosen as a quality control margin.

[1]The fraction of textured 111 component can be also determined from measurements of 222 rocking curves and constructing the product EF_{222} similar to that given by (1). The PF can then be estimated from the area under another (e.g., 440) reflection.

[2]Strictly speaking, $EF + PF < 1$ does not necessarily mean that the rest part is amorphous, but might indicate that LZO partly decomposes. Decomposition of LZO to ZrO_2 plus other phases is observed when annealing LZO/NiW tapes under humid conditions ($DP \geq 22°C$).

Authorized licensed use limited to: Oak Ridge National Laboratory. Downloaded on September 6, 2009 at 11:04 from IEEE Xplore. Restrictions apply.

Nexans has a two-year experience of using estimates of EF and PF for quality control of pre-pilot plant production of LZO buffered NiW tapes. The procedure helped us to identify and solve a number of issues during scaling the MOD process first to the 10 and now to the 50 m length. The examples are the development of double-step process (Fig. 1) that helps to suppress coupling between zones in an RTR system with unidirectional gas flow; the necessity to control low humidity levels during heat treatment (Fig. 2); understanding the effect of postannealing and positive role of controlled moderate humidity (Fig. 5). The described method can be applied to any other layer in the coated conductor architecture. Our current efforts are focused on developing similar tool for multilayer structures, in particular, for $\mathrm{MOD-CeO_2/MOD-LZO}$ buffered Ni-5%W RABITS.

Assessment of EF in LZO buffered long length conductors produced in the RTR system currently consists in analyzing head and tail samples cut from the required length until the same EF (>80%) values are obtained. The experience of producing over 500 m of cumulative length of LZO buffered NiW shows that this is in general sufficient to guarantee similar properties for the rest of the tape. Using a 2D detector should make possible continuous characterization of the whole length.

VII. Conclusion and Outlook

A simple method utilizing XRD and ellipsometry (reflectometry) is developed for quantitative assessment of the epitaxy in buffer layers. Its usefulness for quality control of LZO-buffered NiW RABITS is demonstrated.

A good epitaxy is the necessary, but not the only parameter controlling the quality of LZO buffer layer. Surface roughness [7], layer porosity [8], degree of pyrochlore ordering [9] may affect the final performance. The work is under way for developing quantitative criteria for those properties and imposing quality margins by analyzing correlation to final performance. In addition, the functional properties of LZO layer to suppress Ni diffusion to YBCO and minimize oxidation of NiW substrates should be tuned to the parameters of particular YBCO deposition process through adjusting layer thickness. Possible effects of changing the thickness on the quality of the layer have to be studied.

Appendix

The volume V of material can be estimated from the scattering intensity $I(q)$: $V \sim \int d^3qI(q) = \int L(\omega,\theta)I(2\theta,\omega,\chi)d(2\theta)d\omega d\chi$, where $L(\omega,\theta) = (2/\lambda)\cos\omega.\cos\theta$. For epitaxial grains [sharp $I(2\theta,\omega,\chi)$], $L(\omega,\theta) \approx L = \mathrm{const}$. Using integral breadths $\Delta\omega$ and $\Delta\chi$, one can write $V \sim L\Delta\omega\Delta\chi A$, where A is the area under the $\theta - 2\theta$ scan.

The 100 epitaxial fraction of LZO, EF_{400}, can then be determined by comparing $\Delta\omega\Delta\chi A_{400}$ for the sample in question (subscript S) and a perfect sample (subscript P) with 100% epitaxial LZO. Taking into account the difference in thickness d of the layers, we have

$$EF_{400} = \gamma \frac{A_{400}^S \left\{1 - \exp\left[-2\mu d_P/\sin(\theta)\right]\right\} \Delta\omega_S \Delta\chi_S}{A_{400}^P \left\{1 - \exp\left[-2\mu d_S/\sin(\theta)\right]\right\} \Delta\omega_P \Delta\chi_P},$$

where μ is the linear absorption coefficient, and γ is the factor accounting for the differences in geometry of XRD measurements (illuminated area, beam intensity, etc).

This formula is valid for any fixed φ. When $\Delta\omega(\varphi)$ is larger than the resolution in χ, $\Delta\chi(\varphi) = \Delta\omega(\varphi + 90°)$. In RABITS tapes, there are two distinct φ values corresponding to the scan axis along the rolling (RD) and transverse (TD) directions. As both corresponding breadths $\Delta\omega^{(\mathrm{RD})}$ and $\Delta\omega^{(\mathrm{TD})}$ of the ω scans are larger than 2.5° (the resolution in χ of our instrument), we have used two ω scans instead of ω and χ. The formula for EF is then transformed to expression (1) in the text.

Expression (2) for the polycrystalline fraction PF is self explanatory. It is assumed that no preferred orientation exists in that part of the layer.

Error propagation for EF and PF is straightforward. For a diffractometer setting leading to the intensity of 101 $\mathrm{SiO_2}$ powder sample (particle size 3 μm) $I(26.64°) \approx 4500$ cps, the relative accuracy of 5% for EF of 100 nm thick film is achieved in ~30 min measurements.

Acknowledgment

The authors thank Prof. Philippe Odier (CNRS, Grenoble, France) for stimulating discussions and Bernhard Hoppe, Nikolai Berenzon, Jochen Schütz, and Shylate Mahachi (Nexans SuperConductors) for help in the experiments.

References

[1] A. Rar, J. Reeves, and V. Selvamanickam, "Advanced characterization supporting the manufacture of long lengths of high performance 2G HTS wire at SuperPower," in *CEC/ICMC 2007*, Chattanooga, TN [Online]. Available: http://www.superpower-inc.com

[2] S. Sathyamurthy, M. Paranthaman, T. Aytug, B. W. Kang, P. M. Martin, A. Goyal, D. M. Kroeger, and D. K. Christen, "Chemical solution eposition of lanthanum zirconate buffer layers on biaxially textured Ni-1.7%Fe-3%W substrates for coated conductor fabrication," *J. Mater. Res.*, vol. 17, pp. 1543–1549, 2002.

[3] E. D. Specht and F. A. List, "Texture by the kilometer," in *Materials for High-Temperature Superconductor Technologies*, M. Paranthaman, M. W. Rupich, K. Salama, J. Mannhart, and K. Hasegawa, Eds. Warrendale, PA: Materials Research Society, 2002, vol. 689, Mat. Res. Soc. Symp. Proc., pp. 277–282.

[4] B. Utz, R. Semerad, M. Bauer, W. Prusseit, P. Berberich, and H. Kinder, "Deposition of YBCO and NBCO films on areas of 9 inches in diameter," *IEEE Trans. Appl. Supercond.*, vol. 7, no. 2, pp. 1272–1275, 1997.

[5] S. Sathyamurthy, K. Kim, T. Aytug, and M. Paranthaman, "Effect of relative humidity on the crystallization of sol-gel lanthanum zirconium oxide films," *Chem. Mater.*, vol. 18, no. 25, pp. 5829–5831, 2006.

[6] W. W. Schmahl, M. Lehmann, S. Räth, M. Gerards, and R. Riddle, "An improved method to determine the weight fraction of 2212 and 2201 phase impurities in BSCCO-2223 powders from x-ray powder diffraction peaks," *Supercond. Sci. Technol.*, vol. 11, no. 12, pp. 1269–1276, Dec 1998.

[7] K. Knoth, R. Hühne, S. Oswald, L. Schultz, and B. Holzapfel, "Detailed investigations on $\mathrm{La_2Zr_2O_7}$ buffer layers for YBCO-coated conductors prepared by chemical solution deposition," *Acta Materialia*, vol. 55, no. 2, pp. 517–529, Feb. 2007.

[8] L. Molina, K. Knoth, S. Engel, B. Holzapfel, and O. Eibl, "Chemically deposited $\mathrm{La_2Zr_2O_7}$ buffer layers for YBCO-coated conductors: Film growth and microstructure," *Supercond. Sci. Technol.*, vol. 19, no. 11, pp. 1200–1208, Nov. 2006.

[9] J. T. Caroff, S. Morlens, A. Abrutis, M. Decroux, P. Chaudouèt, L. Porcar, Z. Saltyte, C. Jiménez, P. Odier, and F. Weiss, " $\mathrm{La_2Zr_2O_7}$ single buffer layer for YBCO RABiTS coated conductors," *Supercond. Sci. Technol.*, vol. 21, no. 7, p. 075007, July 2008, 8pp.

Authorized licensed use limited to: Oak Ridge National Laboratory. Downloaded on September 6, 2009 at 11:04 from IEEE Xplore. Restrictions apply.